

DOI:10.1002/ejic.201402139

Aerial CO₂ Trapped as CO₃²⁻ Ions in a Dimeric Capsule That Efficiently Extracts Chromate, Sulfate, and Thiosulfate from Water by Anion-Exchange Metathesis

Ranjan Dutta,^[a] Sourav Chakraborty,^[a] Purnandhu Bose,^{[a],[‡]} and Pradyut Ghosh*^[a]

Keywords: Environmental chemistry / Carbon dioxide fixation / Ion exchange / Anions / Liquid–liquid extraction / Sulfates / Chromates

The tris(2-aminoethyl)amine-based (tren-based) 3-cyanophenyl-substituted tripodal urea **L1**, one of the familiar urea-based anion receptors, has shown encapsulation of CO₃²⁻ ions as the carbonate capsule [(**L1**)₂·(CO₃)·(TBA)₂] (**1**, TBA = tetrabutylammonium) by the fixation of aerial carbon dioxide from basic dimethyl sulfoxide (DMSO) solution. Single-crystal X-ray structural analysis confirmed the encapsulation of CO₃²⁻ ions in the cavity of a dimeric capsular assembly of **L1** (9.62 Å) through the formation of twelve strong N–H···O hydrogen-bonding interactions. The excellent CHCl₃ and CH₂Cl₂ solubility of **1** has been exploited for the liquid–liquid (L–L) extraction of CrO₄²⁻, SO₄²⁻, and S₂O₃²⁻ ions from water by anion-exchange metathesis. The extraction of these anions from water was unambiguously confirmed by ¹H NMR spectroscopy, IR spectroscopy, powder XRD (PXRD), and single-crystal X-ray diffraction analysis. The ¹H NMR spectroscopic analysis of the bulk extracts supports the formation of 2:1 (host–guest) complexes. For the CrO₄²⁻ ion, the ⁵³Cr NMR spectrum of the bulk extract shows a characteristic

peak at δ = –99.98 ppm. The complexes of CrO₄²⁻, S₂O₃²⁻, and SO₄²⁻ ions with **L1** (i.e., **2–4**, respectively) were obtained from crystallization of the bulk extracts and show anion-assisted dimeric capsular assemblies of **L1** through multiple N–H···X (X = O, S) interactions. The dimensions of the anion-encapsulated capsular assemblies are quite similar to that of the carbonate capsule and are 9.70 Å for [(**L1**)₂·(CrO₄)·(TBA)₂] (**2**), 9.61 Å for [(**L1**)₂·(S₂O₃)·(TBA)₂] (**3**), and 9.71 Å for [(**L1**)₂·(SO₄)·(TBA)₂] (**4**). Quantification by weighing the bulk extract shows that **1** can separately extract ca. 90 % of the above three anions from water by anion-exchange metathesis. The quantitative estimations of the extractions of SO₄²⁻ and CrO₄²⁻ ions were further verified by gravimetric analysis by BaSO₄ and BaCrO₄ precipitation techniques, respectively. The extraction of SO₄²⁻ ions from water was also demonstrated under alkaline conditions (pH 12.5) and in the presence of an excess of nitrate ions. Further, the quantification of CrO₄²⁻ extraction was established by solution-state UV/Vis studies.

Introduction

Anions in groundwater, specifically a few inorganic oxyanions, can be toxic to human health even at submicromolar concentrations. The contamination of drinking water by CrO₄²⁻ ions can induce respiratory cancer and can affect the gastrointestinal tract, immune system, liver, and kidneys.^[1] The current recommended by the World Health Organization (WHO) for Cr^{VI} ions in drinking water is a maximum level of 0.05 mg L⁻¹.^[2] The removal of SO₄²⁻ ions from radioactive nuclear waste is essential for the improved

vitrification of the waste, and excess SO₄²⁻ ions are also responsible for permanent hardness of water.^[3] On the other hand, S₂O₃²⁻ ions are beneficial in various biological and human health aspects. In addition to the therapeutic use of sodium thiosulfate, thiosulfate ions have recently been used as an antidote for the treatment of cyanide poisoning.^[4] Thus, the liquid–liquid separation of the environmentally and biologically relevant CrO₄²⁻, SO₄²⁻, and S₂O₃²⁻ anions, which have similar H-bonding properties, is very important.

Metal–organic frameworks (MOFs), organic cages, zeolites, and amines have been widely explored for the removal and storage of CO₂.^[5] A few synthetic anion receptors are useful for aerial CO₂ fixation through its conversion to CO₃²⁻ anions. Gale et al. have shown the fixation of aerial CO₂ as CO₃²⁻ anions by amidourea macrocycles and acyclic amine anion receptors from basic dimethyl sulfoxide (DMSO) solutions.^[6] Three other synthetic anion receptors for the fixation of aerial CO₂ as CO₃²⁻ anions under similar reaction condition have also been described.^[7] On the other

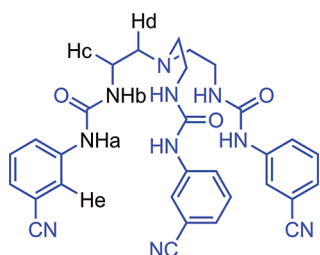
[a] Department of Inorganic Chemistry, Indian Association for the Cultivation of Science, 2A & 2B Raja S.C. Mullick Road, Kolkata 700032, India
E-mail: icpg@iacs.res.in
http://www.iacs.res.in/inorg/icpg

[‡] Current address: Division of Chemistry and Biological Chemistry, School of Physical and Mathematical Sciences, Nanyang Technological University, SPMS-CBC-02-01, 21 Nanyang Link, 637371 Singapore

Supporting information for this article is available on the WWW under <http://dx.doi.org/10.1002/ejic.201402139>.

hand, the design of anion receptors for the extraction of anions such as CrO_4^{2-} and SO_4^{2-} from water is highly challenging owing to the large hydration energies of CrO_4^{2-} ($\Delta G_h = -950 \text{ kJ mol}^{-1}$) and SO_4^{2-} ions ($\Delta G_h = -1080 \text{ kJ mol}^{-1}$).^[8] Absorbents, resins, and membranes are popular for the removal of toxic Cr^{VI} ions from water, but the drawbacks of such systems are their poor selectivity and slow process kinetics.^[9] A few calixarene-based anion receptors have been employed for the extraction of CrO_4^{2-} and $\text{Cr}_2\text{O}_7^{2-}$ anions from water.^[10] Custelcean et al. have shown the selective removal of CrO_4^{2-} anions from water by a self-assembled metal–organic framework by a crystallization technique.^[11] However, the industrial use of L–L extraction processes for the removal of CrO_4^{2-} anions from water is challenging. Since the first report on the transfer of sulfate anions across the interface between two immiscible solvents by Teramae and co-workers,^[12] different strategies have been employed for the extraction of SO_4^{2-} anions from aqueous media over the years.^[13] Sessler, Moyer et al. widely utilized a dual-host and ion-exchange strategy for SO_4^{2-} anion extraction.^[14] A neutral hexakis(urea) receptor and a trithiourea receptor for the extraction of sulfate anions from aqueous environments with tetrabutylammonium chloride and iodide, respectively, as phase-transfer agents have been demonstrated by Wu et al. and our group.^[15] Our group has also shown the efficient and quantitative extraction of SO_4^{2-} ions by employing L–L extraction techniques that utilize the carbonate capsule of a pentafluorophenyl-attached tripodal tris(urea) receptor as an extractant.^[16]

Tris(2-aminoethyl)amine-based (tren-based) urea and thiourea compounds are an intriguing class of anion receptors, particularly for tetrahedral oxyanions.^[17] In 2005, Custelcean et al. reported a tren-based 3-cyanophenyl-functionalized urea receptor (**L1**) for the encapsulation of SO_4^{2-} ions in a metal–organic framework, and we have recently shown the encapsulation of staggered oxalate ions by **L1** (Scheme 1).^[17b,17p] Herein, we report the utilization of **L1** for the encapsulation of CO_3^{2-} ions in its dimeric capsular assembly by the tetrabutylammonium hydroxide (TBAOH) induced fixation of aerial CO_2 . Further, we have shown the efficient extraction of CrO_4^{2-} , SO_4^{2-} , and $\text{S}_2\text{O}_3^{2-}$ ions from water by the above carbonate capsule by an L–L extraction process. The SO_4^{2-} anion extraction properties of the carbonate capsules of **L1** and **L2** (Scheme S1, Supporting Information) under alkaline conditions are also compared. Structural analysis reveals anion-assisted dimeric assemblies



Scheme 1. Chemical structure of the receptor **L1**.

of **L1** through multiple N–H···X (X = O/S) interactions for all anion complexes. To the best of our knowledge, this represents the first report on the efficient L–L extraction of CrO_4^{2-} and $\text{S}_2\text{O}_3^{2-}$ ions by an anion-exchange strategy.

Results and Discussion

The 3-cyanophenyl-substituted urea receptor **L1** was synthesized by the literature procedure.^[17b] Crystals of **1** were isolated in high yield (85%) by the addition of TBAOH to a DMSO solution of **L1**. We have previously reported the synthesis of **L2** and its CO_3^{2-} complex.^[7b,17d] Crystals of **2–4** were isolated from the crystallization of the extracted solid in DMSO and also by the reaction of **L1**, TBAI, and the corresponding sodium salt in DMSO/ H_2O (19:1). The structures of **2–4** are discussed in the last section.

Fixation of Aerial CO_2

In our previous communication, we have reported the efficient capture of aerial CO_2 in the form of CO_3^{2-} anions by **L2**.^[7b] In our continuing search for new and alternate systems, we have found the sequestration of aerial CO_2 as CO_3^{2-} ions by TBAOH and subsequent encapsulation of the CO_3^{2-} ions in the dimeric capsular assembly of **L1** in DMSO. When TBAOH was added to a DMSO solution of **L1** in an open container, diamond-shaped crystals of $[(\text{L1})_2 \cdot (\text{CO}_3)_2 \cdot (\text{TBA})_2]$ (**1**) were obtained within 2–3 d in high yield (85%). The crystallization of **1** occurs at the air–solvent (DMSO) interface at which the CO_2 concentration is higher (Figure S1). The high-yield generation of carbonate capsules indicates the high encapsulating affinity of **L1** towards in situ generated CO_3^{2-} ions. The structural analysis of **1** shows the encapsulation of a CO_3^{2-} ion in the cavity of a dimeric capsular assembly of **L1** with a dimension of 9.62 Å (Figures 1 and S26). Each oxygen atom of the encapsulated CO_3^{2-} ion (i.e., O7, O8, and O9) is involved in four N–

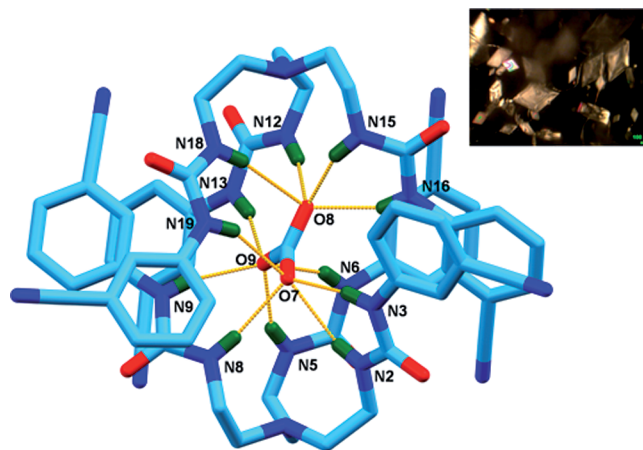


Figure 1. Molecular structure of **1** showing the complete encapsulation of a CO_3^{2-} ion inside the dimeric assembly of **L1** through twelve N–H···O interactions. The diamond-shaped crystals of **1** are shown in the inset (nonacidic hydrogen atoms and counterions are omitted for clarity).

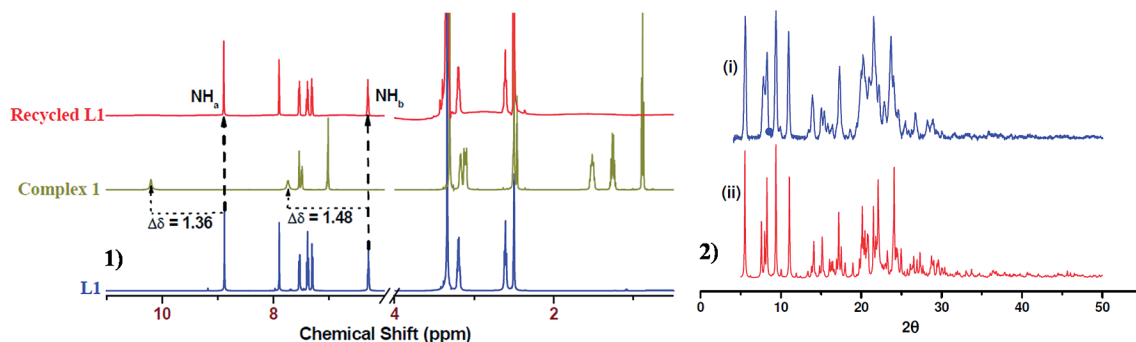


Figure 2. (1) The ^1H NMR spectra of **L1**, **1**, and recycled **L1** formed by methanol/water (1:4 v/v) treatment. (2) (i) Simulated and (ii) experimental PXRD patterns of **1**.

$\text{H}\cdots\text{O}$ hydrogen-bonding interactions with the $-\text{NH}$ group of **L1**, which results in a total of twelve strong H-bonding interactions in **1** (Figure 1). In **L2**, thirteen such strong H-bonding interactions were observed upon CO_3^{2-} ion encapsulation, and the capsular dimension is smaller (9.17 Å).^[7b] The $\text{N}\cdots\text{O}$ bond lengths ranges from 2.78 to 3.21 Å in **1**, whereas the $\text{N}-\text{H}\cdots\text{O}$ bond angles are 145 to 171°. Details of the hydrogen-bonding parameters and a scatter plot are presented in the Supporting Information (Figure S27 and Table S2). The ^{13}C NMR spectrum of **1** shows a signal at $\delta = 169.72$ ppm, which corresponds to the carbon atom of the encapsulated CO_3^{2-} ion. The downfield shift of 11 ppm compared with the resonance of the free CO_3^{2-} ion of tetraethylammonium hydrogen carbonate indicates that the CO_3^{2-} ion is strongly bound in the dimeric capsular assembly of **1** (Figure S12). The purity of the bulk material of the carbonate capsules was verified by powder X-ray diffraction; the simulated and experimental diffraction patterns are similar (Figure 2). Similarly to **L2**, **L1** can also be easily recycled by treating **1** with a methanol/water (1:4) mixture (Figures 2, S2, and S11).^[7b] First, **1** was dissolved in MeOH in a test tube to give a clear solution, which became turbid after the addition of water. After the solution had settled, a colorless precipitate deposited. The comparative IR data of the solid shows the absence of CO_3^{2-} stretching frequencies, and the spectral pattern is similar to that of pure **L1**. Further, the ^1H NMR spectra of the recycled solid, **1**, and **L1** show the recovery of pure **L1** from **1** upon MeOH/ H_2O treatment. Almost quantitative (95%) recovery of **L1** from **1** is estimated by this technique. This recycled **L1** was further reacted with TBAOH in DMSO to obtain crystals of **1** in a yield of more than 80%.

Liquid–Liquid Extraction Studies

The quantitative formation of **1** and its solubility in water-immiscible solvents such as CHCl_3 and CH_2Cl_2 encouraged us to investigate the L–L extraction by **1** of anions such as CrO_4^{2-} , $\text{S}_2\text{O}_3^{2-}$, SO_4^{2-} , H_2PO_4^- , HAsO_4^{2-} , and F^- from water. We found that the extraction of CrO_4^{2-} , $\text{S}_2\text{O}_3^{2-}$, and SO_4^{2-} ions by **1** by anion-exchange metathesis was efficient. However, the extraction of H_2PO_4^- , HAsO_4^{2-} and F^- ions by **1** was unsuccessful. On the other hand, the

carbonate complex of **L2** is only capable of the extraction of SO_4^{2-} ions among all of the above anions. The details of the L–L extraction studies and characterization techniques are described below.

In a typical extraction experiment, **1** (1 mmol) was dissolved in CH_2Cl_2 (5 mL), followed by the addition of deionized water (5 mL) containing K_2CrO_4 (10 equiv., ca. 10^{-2} M). The aqueous–organic biphasic solution was then stirred for 6 h at room temp. Upon L–L extraction, the organic phase appeared yellow. The mixture was then allowed to settle for half an hour, and the organic layer was filtered through silicone-treated Whatmann 1PS filter paper. The evaporation of the organic layer yielded a bright yellow solid, which crystallized from DMSO as $[(\text{L1})_2 \cdot (\text{CrO}_4) \cdot (\text{TBA})_2]$ (**2**). The ^1H NMR spectroscopic analysis of the crude solid extract shows upfield shifts of 0.85 ppm for NH_a and 0.63 ppm for NH_b with respect to the values for **1**; the shifts are the same as those for crystals of **2** (Figure 3, a). Further, the integration of the signals of the CH_e proton of **L1** and the CH_8 proton of the TBA group suggest a 2:1 (host–guest) stoichiometry in the extracted solid (Figure S13). Thus, the pure extraction of CrO_4^{2-} ions is clearly evident from the ^1H NMR spectroscopic study. The ^{53}Cr NMR spectrum of the extracted solid in $[\text{D}_6]\text{DMSO}$ shows a peak at $\delta = -99.98$ ppm, which is characteristic of bound CrO_4^{2-} ion, compared to the standard ^{53}Cr NMR signal of K_2CrO_4 in D_2O at $\delta = 0$ ppm (Figure S15). The UV/Vis spectra of crystals of **2** and the bulk CrO_4^{2-} extract in acetonitrile show a characteristic CrO_4^{2-} peak at 372 nm. Similar absorbance values [optical density (OD) = 0.53] were observed for both **2** and the bulk extract at the same experimental concentrations; this further supports the purity of the extraction from water (Figure 3, b). The amount of CrO_4^{2-} ions was estimated both by weighing the bulk extract and by gravimetric analysis. Simple weighing of the bulk extract shows ca. 94% extraction of CrO_4^{2-} ions (with respect to **1**) from water (Table S6). Gravimetric analysis of the CrO_4^{2-} ion extraction was performed by BaCrO_4 precipitation upon the addition of aqueous BaCl_2 to the CH_2Cl_2 solution of the bulk extract; the amount of CrO_4^{2-} ions extracted by **1** was calculated to be >90% (Table S6). Moreover, the similarity of the powder XRD (PXRD) pattern of the bulk extract and the simulated pattern of

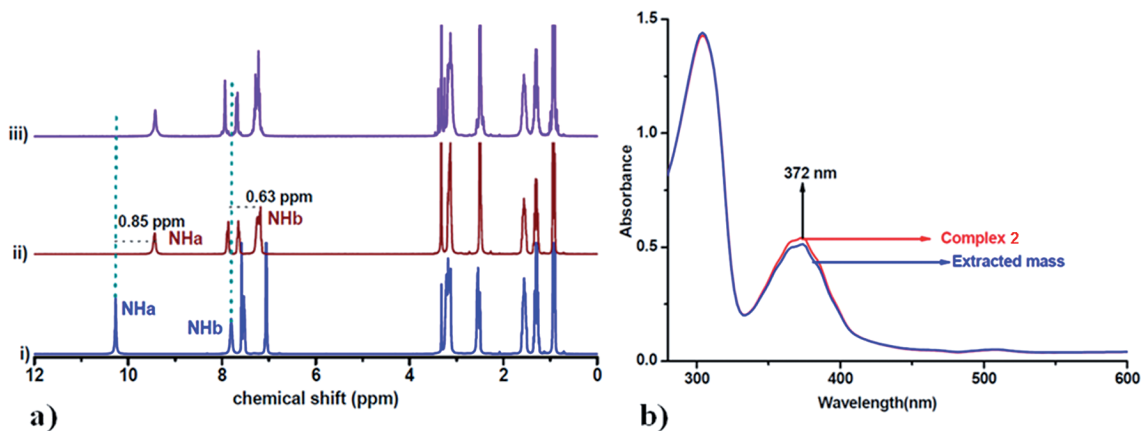


Figure 3. (a) ^1H NMR spectra of (i) **1**, (ii) **2**, and (iii) bulk extract. (b) UV/Vis spectra of **2** and bulk extract.

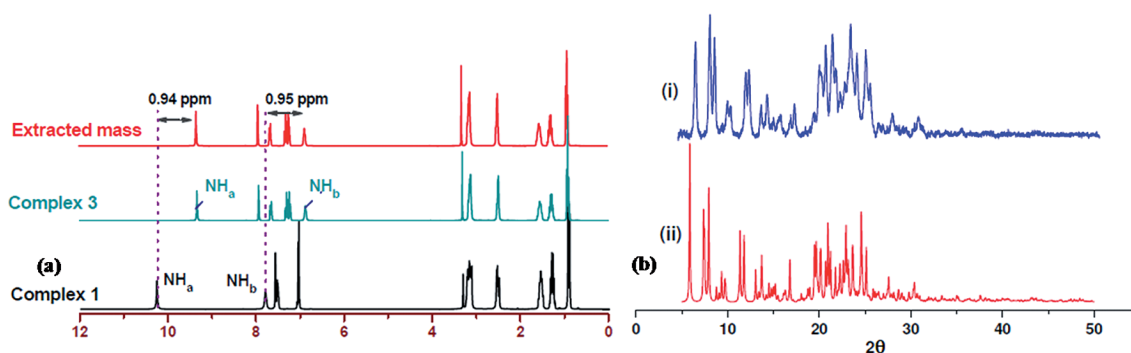


Figure 4. (a) ^1H NMR spectra of (i) **1**, (ii) **3**, and (iii) bulk extract. (b) PXRD patterns of (i) **3** (simulated) and (ii) bulk extract (experimental).

crystals of **2** supports the purity of the bulk extract (Figure S14). In a similar fashion, water (5 mL) containing $\text{Na}_2\text{S}_2\text{O}_3$ (10 equiv.) was added to a solution of **1** (1 mmol) in dichloromethane (DCM, 5 mL). After the usual extraction and workup, the bulk extract was characterized by ^1H NMR spectroscopy, PXRD analysis, and single-crystal X-ray structure analysis. The ^1H NMR spectrum of the bulk extract shows signals for NH_a and NH_b at $\delta = 9.34$ and 6.88 ppm, respectively, compared with $\delta = 10.27$ and 7.80 ppm for **1**. The single crystal of $[(\text{L}1)_2 \cdot (\text{S}_2\text{O}_3) \cdot (\text{TBA})_2]$ (**3**) obtained from DMSO shows a very similar ^1H NMR spectrum to that of the bulk extract (Figure 4, a). Again, the integration of the signal of the CH_c proton of **L1** and the CH_δ proton of TBA indicates a 2:1 (host-guest) stoichiometry in the bulk $\text{S}_2\text{O}_3^{2-}$ extraction product (Figure S16). The purity of the bulk extract was confirmed by PXRD analysis (Figure 4, b). An estimation of the amount of $\text{S}_2\text{O}_3^{2-}$ ions extracted by weighing the bulk extract reveals ca. 94% extraction (Table S7).

Like that of CrO_4^{2-} and $\text{S}_2\text{O}_3^{2-}$ ions, the L-L extraction of SO_4^{2-} ions was performed with **1** (1 mmol) in DCM and K_2SO_4 (10 equiv.) in water. The expected carbonate-sulfate exchange was verified by the pink coloration of the aqueous phase in the presence of phenolphthalein indicator, which confirmed the basic nature of aqueous phase (Figure S17). The bulk extracted solid was then crystallized from DMSO as $[(\text{L}1)_2 \cdot (\text{SO}_4) \cdot (\text{TBA})_2]$ (**4**) and characterized by ^1H NMR

spectroscopy, IR spectroscopy, and single-crystal X-ray diffraction analysis. A comparison of the IR spectra of **1** and the bulk SO_4^{2-} extract shows the disappearance of the peak at 1380 cm^{-1} and the appearance of a new peak at 1121 cm^{-1} , which corresponds to the stretching frequency of SO_4^{2-} ions (Figure S19). The ^1H NMR spectra of **1**, the bulk SO_4^{2-} extract, and **4** are presented in Figure 5. The ^1H NMR spectra of **1** and the bulk extract show chemical shift changes of the parent NH_a signal from $\delta = 10.27$ to 9.46 ppm and the NH_b signal from $\delta = 7.80$ to 7.24 ppm. Similar chemical shifts of the signals of the urea NH_a and NH_b protons were observed in the ^1H NMR spectra of **4**, which suggests that the extraction of SO_4^{2-} ions by anion-exchange metathesis proceeds cleanly (Figure 5, a). Importantly, the integration of the signals of CH_c of **L1** and CH_δ of the tetrabutylammonium cation indicate a 2:1 **L1**/ SO_4^{2-} ratio in the extracted solid (Figure S17). Further, the purity of the bulk extract was confirmed by the resemblance of its PXRD pattern with the simulated pattern of the single crystals of **4** (Figure 5, b). Finally, the quantification of SO_4^{2-} ion extraction was performed by simple weighing of the extracted mass after L-L extraction. This suggested that ca. 95% of the SO_4^{2-} ions were extracted (Table S8). Further, the extent of the SO_4^{2-} ion extraction was verified by precipitation of BaSO_4 from the bulk extract by the addition of an aqueous BaCl_2 solution to a CH_2Cl_2 solution of the bulk extract. The gravimetric analysis of the isolated BaSO_4

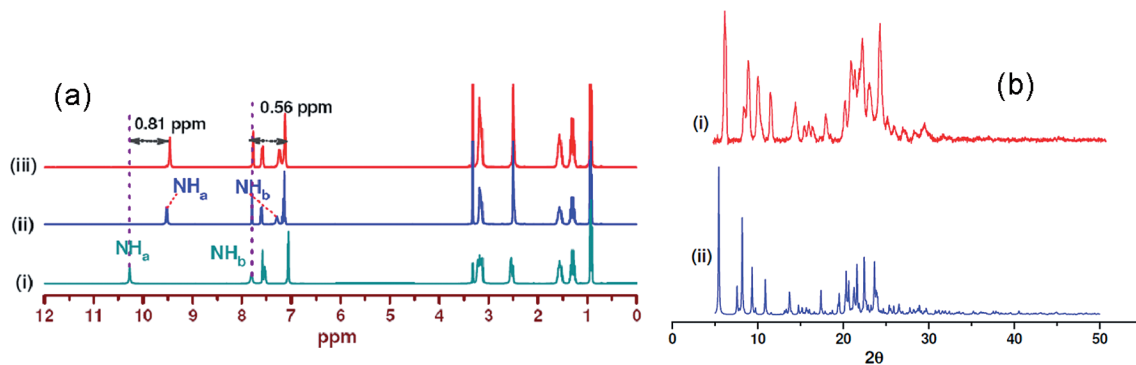


Figure 5. (a) ¹H NMR spectra of (i) **1**, (ii) **4**, and (iii) bulk extract. (b) PXRD patterns of (i) **4** (simulated) and (ii) bulk extract (experimental).

also shows the high efficiency of the extraction. To verify the extraction ability of **1** in the presence of 1 equiv. of anions, the above extraction method was repeated in the presence of a 1:1 stoichiometric ratio of **1** and the respective anions. The average extraction efficiency of **1** towards all three anions was ca. 90% (Table S9–11S). In all cases, a slightly lower extraction percentage was observed by this process. Moreover, we tested the extraction ability of **1** towards CrO₄²⁻ ions at lower concentration and found that **1** can extract CrO₄²⁻ ions at 10⁻⁵ M in water; however, the CrO₄²⁻ ion concentration in drinking water is much lower than this.

Additionally, we have studied the extraction of SO₄²⁻ ions by **1** in highly alkaline media, which is required for the practical application of the separation of SO₄²⁻ ions from nuclear waste for improved vitrification. We maintained the pH of an aqueous solution of K₂SO₄ by adding NaOH solution and then performed the usual L–L extraction experiment under increasingly alkaline condition. Interestingly, the clean and efficient extraction of SO₄²⁻ ions from water by **1** to pH 12.5 was successfully observed by comparative ¹H NMR spectral analysis (Figure 6, a). In this context, Custelcean et al. have employed a crystallization approach for the removal of SO₄²⁻ ions with high efficiency under highly alkaline conditions.^[17n] Complex **1** also shows the clean extraction of SO₄²⁻ ions in the presence of 5 equiv. of NO₃⁻ ions (Figure S20). We also extended our study towards the extraction of SO₄²⁻ ions at alkaline pH to the

CO₃²⁻ complex of **L2** and found that the CO₃²⁻ complex of **L2** can extract SO₄²⁻ ions from water only up to pH 10.5. The bulk extract for **L2** was also characterized by IR spectroscopy, ¹H NMR spectroscopy, and single-crystal X-ray crystallography. The comparative IR study shows the disappearance of the stretching frequency at 1370 cm⁻¹ for the bulk extract, as observed previously (Figure S21). The ¹H NMR spectrum of the bulk extract in [D₆]DMSO reveals upfield shifts of both NH_a (Δδ = 0.97 ppm) and NH_b (Δδ = 0.73 ppm) compared with the resonances of the parent CO₃²⁻ complex (Figure 6, b). Very similar chemical shifts for the NH_a and NH_b protons were observed for the SO₄²⁻ complex of **L2** in [D₆]DMSO.^[17g] A drawback of the carbonate complex of **L2** towards the extraction of SO₄²⁻ ions is its relatively narrow pH window of extraction activity (Figure S22). On the other hand, in addition to SO₄²⁻ ions, complex **1** can also extract S₂O₃²⁻ and CrO₄²⁻ ions. Interestingly, complex **1** can extract SO₄²⁻ ions more effectively than the CO₃²⁻ complex of **L2** under highly alkaline conditions (pH 12.5), which are more relevant for practical applications of SO₄²⁻ separation. Similar to those with **1**, recycling experiments were performed with **2–4** to recover **L1**. In all three cases, we recovered pure **L1** upon treatment with MeOH/H₂O (1:4 v/v; Figure S23–S25). A comparison of the ¹H NMR spectroscopic data supports the regeneration of pure **L1** from the complexes in good yield. A 75% recovery of pure **L1** is estimated for **4**, whereas ca. 80% recovery of **L1** is calculated for **2** and **3**.

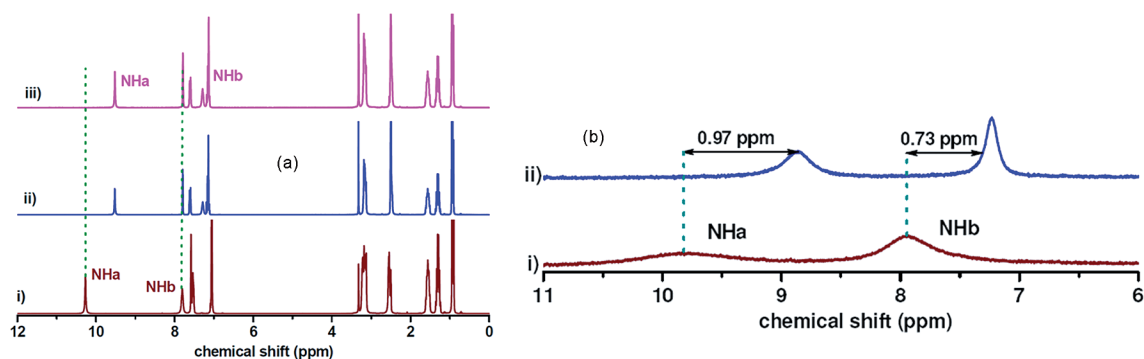


Figure 6. (a) ¹H NMR spectra of (i) **1**, (ii) **4**, and (iii) the bulk SO₄²⁻ extract at pH 12.5. (b) ¹H NMR spectra of the carbonate capsule of **L2** and the bulk SO₄²⁻ extract at pH 10.5 in [D₆]DMSO.

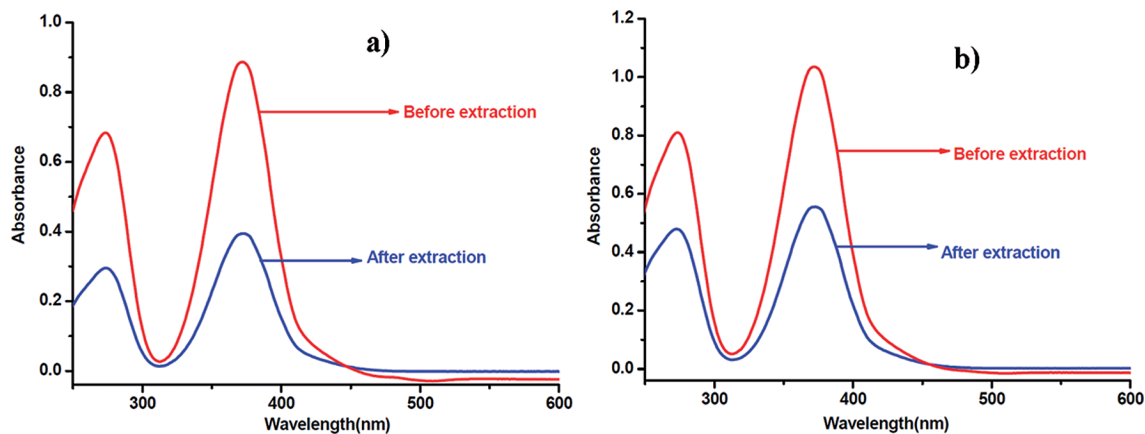


Figure 7. UV/Vis spectral analysis of (a) CrO_4^{2-} ion extraction by **1** [absorbance (A) = 0.8868 and 0.3942 at 372 nm before and after extraction, respectively. Conc. of CrO_4^{2-} before extraction = 2.49×10^{-4} M] and (b) CrO_4^{2-} ion extraction from a 1:1 mixture of K_2CrO_4 and K_2SO_4 [A = 1.0354 and 0.5553 at 372 nm before and after extraction, respectively. Conc. of CrO_4^{2-} before extraction = 2.48×10^{-4} M].

CrO_4^{2-} Ion Extraction and Selectivity Study by UV/Vis Spectroscopic Analysis

Additionally, solution-state UV/Vis studies were performed to allow estimation of the amount of CrO_4^{2-} ions extracted by **1**. The details of this study are described in the Supporting Information. In this case, ca. 1.2 equiv. of K_2CrO_4 (relative to **1**) was dissolved in water during the extraction. First, we measured the absorbance of the aqueous CrO_4^{2-} solution before the L–L extraction study. Then, upon completion of the extraction (ca. 6 h), the absorbance of the aqueous layer was measured again. By this method, we estimated the amount of CrO_4^{2-} ions removed during the L–L extraction, and our calculation shows ca. 70% extraction of CrO_4^{2-} ions from water with respect to **1** (Figure 7, a). The same experiment was performed to estimate the amount of CrO_4^{2-} ions removed by **1** from a mixture of CrO_4^{2-} and SO_4^{2-} ions. The UV/Vis spectral calculations revealed ca. 50% extraction of CrO_4^{2-} ions from the mixture (Figure 7, b).

Solution-State ^1H NMR Titration Study for **L1**

The solution-state binding of **L1** with CO_3^{2-} , CrO_4^{2-} , $\text{S}_2\text{O}_3^{2-}$, and SO_4^{2-} ions was studied by ^1H NMR titration. For CO_3^{2-} ions, a solution of **L1** in $[\text{D}_6]\text{DMSO}$ was titrated

against a solution of tetraethylammonium hydrogen carbonate (TEAHCO_3) in $[\text{D}_6]\text{DMSO}$. On the other hand, for CrO_4^{2-} , $\text{S}_2\text{O}_3^{2-}$, and SO_4^{2-} ions, a solution of **L1** in $[\text{D}_6]\text{DMSO}/\text{D}_2\text{O}$ (9:1 v/v) was titrated against solutions of the anions as their sodium salts in a $[\text{D}_6]\text{DMSO}/\text{D}_2\text{O}$ (1:1.1 v/v) solvent mixture. For the titration of **L1** with CO_3^{2-} ions, we observed downfield shifts of the NH_a and NH_b signals and an upfield shift of the signal of CH_d (Figure 8, a). Upon the gradual addition of CO_3^{2-} ions, a broadening of the NH_a and NH_b signals was observed with the disappearance of the NH_a signal. Upfield shifts of 2.61 to 2.5 ppm were observed for CH_d upon the addition of ca. 1 equiv. of CO_3^{2-} ions. A Job plot analysis of the upfield shift of CH_d reveals that there is 1:1 (host–guest) binding between **L1** and CO_3^{2-} (Figure 8, b). This discrepancy of 1:1 (host–guest) binding in solution and 2:1 (host–guest) binding in the solid state is common for tripodal urea and thiourea receptors.^[17,17p]

The binding constant ($\log K$) for **L1** with CO_3^{2-} ions was calculated as 3.12 by using the WINEQ/NMR software.^[18] In this context, **L2** shows a $\log K$ value of 4.04 with CO_3^{2-} ions in $[\text{D}_6]\text{DMSO}$ as determined by ^1H NMR titration. For CrO_4^{2-} , $\text{S}_2\text{O}_3^{2-}$, and SO_4^{2-} ions, upfield shifts of the signals of the CH_c and CH_d protons and the disappearance of the signal of the NH_a and NH_b protons were observed

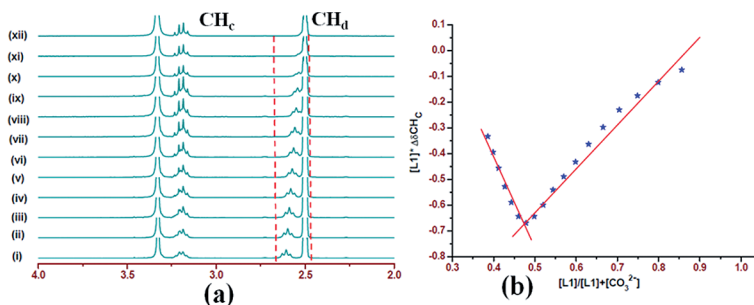


Figure 8. (a) Partial ^1H NMR spectral changes for the titration of **L1** (5.18 mM) in $[\text{D}_6]\text{DMSO}$ and standard TEAHCO_3 (25.99 mM) in $[\text{D}_6]\text{DMSO}$ (298 K). $[\text{TEAHCO}_3]/[\text{L1}]$: (i) 0, (ii) 0.08, (iii) 0.16, (iv) 0.24, (v) 0.32, (vi) 0.40, (vii) 0.48, (viii) 0.56, (ix) 0.64, (x) 0.72, (xi) 1.12, (xii) 1.20. (b) Job plot for **L1** with TEAHCO_3 in $[\text{D}_6]\text{DMSO}$.

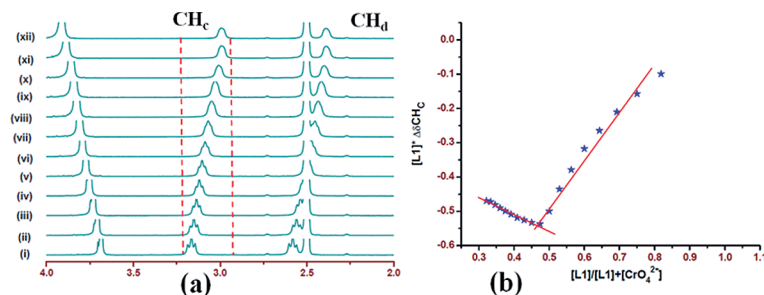


Figure 9. (a) Partial ^1H NMR spectral changes for the titration of **L1** (3.66 mM) in $[\text{D}_6]\text{DMSO}/\text{D}_2\text{O}$ (9:1 v/v) and standard K_2CrO_4 (25.4 mM) in $[\text{D}_6]\text{DMSO}/\text{D}_2\text{O}$ (1:1.1) at 298 K. $[\text{CrO}_4^{2-}]/[\text{L1}]$: (i) 0, (ii) 0.11, (iii) 0.22, (iv) 0.33, (v) 0.44, (vi) 0.55, (vii) 0.67, (viii) 0.78, (ix) 0.89, (x) 0.99, (xi) 1.11, (xii) 1.22. (b) Job plot for **L1** with K_2CrO_4 in $[\text{D}_6]\text{DMSO}/\text{D}_2\text{O}$ (1:1.1).

upon the gradual addition of anions. Chemical shift changes ($\Delta\delta$) of 0.17 and 0.13 ppm for CH_c were observed for the addition of ca. 1 equiv. of CrO_4^{2-} and $\text{S}_2\text{O}_3^{2-}$ anions, respectively (see part a of Figure 9 and Figure S29a). An upfield shift of 0.17 ppm ($\Delta\delta$) was found for CH_d upon the addition of ca. 1 equiv. of SO_4^{2-} anions (Figure S30a). A Job plot analysis shows that there is 1:1 (host-guest) stoichiometry between **L1** and all three anions (see part b of Figure 9 and Figures S29b and S30b). One such representative titration profile along with the Job plot for the CrO_4^{2-} ion titration is provided in Figure 9. The binding constant ($\log K$) values were calculated to be ca. 10^4 for **L1** with all three anions.

Mechanism of CO_2 Sequestration and Liquid-Liquid Extraction of CrO_4^{2-} , $\text{S}_2\text{O}_3^{2-}$ and SO_4^{2-} Ions

The formation of CO_3^{2-} ions in DMSO solvent is due to the conversion of aerial CO_2 to CO_3^{2-} in the presence of base (OH^- ions). The conversion of aerial CO_2 to CO_3^{2-} ions is evident from a control experiment. Solid TBAOH was added to $[\text{D}_6]\text{DMSO}$ in the absence of **L1**, and the mixture was kept in open air overnight. The ^{13}C NMR spectrum of the solution shows the appearance of a signal at $\delta = 157.83$ ppm (Figure S31), which indicates the formation of free CO_3^{2-} ions in solution by CO_2 fixation. The good affinity of the receptor towards CO_3^{2-} ions facilitates the formation of the carbonate capsule (**1**) at the liquid-air interface in high yield. The high solubility of **1** in water-immiscible solvents makes **1** a successful L-L extractant. For the L-L extraction of SO_4^{2-} ions with a phase-transfer agent, a 1:1 concentration ratio between the receptor and phase-transfer agent is needed. Often, an excess of phase-transfer agent has to be used to ensure the $\text{CHCl}_3/\text{CH}_2\text{Cl}_2$ solubility of the receptor and, in turn, this may cause impure extraction. However, **1** is a 2:1 complex of **L1** and CO_3^{2-} ions with an exact ratio of tetrabutylammonium counteranions. This balanced feature of the carbonate capsule rules out the possibility of any excess CO_3^{2-} ions (phase-transfer agent) in the organic layer. The combined effect of the higher binding affinity of **L1** towards CrO_4^{2-} , $\text{S}_2\text{O}_3^{2-}$, and SO_4^{2-} ions over CO_3^{2-} ions and the higher hydration energy of CO_3^{2-} ions ($\Delta G_{\text{h}} = -1315 \text{ kJ mol}^{-1}$) over oxyanions such as CrO_4^{2-} and SO_4^{2-} makes anion-exchange

metathesis feasible across water-dichloromethane biphas. This anion-exchange metathesis process results in CO_3^{2-} anions and Na^+ and K^+ cations in the water layer, whereas **L1**, TBA, and CrO_4^{2-} , $\text{S}_2\text{O}_3^{2-}$, and SO_4^{2-} ions are found in the DCM layer. A CH_2Cl_2 solution of the carbonate capsule can exist as an equilibrium mixture of carbonate-bound dimer and monomer; the monomeric species predominates in solution, as ^1H NMR spectroscopy supports stoichiometry of ca. 1:1 in solution. During liquid-liquid extraction, the exchange between CO_3^{2-} and SO_4^{2-} ions occurs because the relatively higher association constant of SO_4^{2-} ions and the higher hydration energy of CO_3^{2-} ions lead to the formation of SO_4^{2-} -bound monomeric and dimeric species of **L1** at the water-chloroform interface. Although, monomeric species may be the dominant species in the equilibrium in solution, the crystallization of the bulk SO_4^{2-} extract results in the isolation of a dimeric capsular assembly of **L1** to satisfy the best packing and higher coordination number of oxyanions such as SO_4^{2-} in the solid state. However, in addition to the characterization of the crude bulk solid of the liquid-liquid extraction experiment, we have examined the anion-exchange phenomenon in solution. For SO_4^{2-} ions as representative case, carbonate capsules (of **L1/L2**) were dissolved in CDCl_3 in an NMR tube. The ^1H NMR spectra of the capsules were then recorded. A D_2O solution of K_2SO_4 was added to the NMR tube, and the mixture was shaken for 5 min; the bilayer was then allowed to settle for a few minutes. A comparison of the ^1H NMR spectra of the settled CDCl_3 layer and **4** in CDCl_3 reveals complete exchange between CO_3^{2-} and SO_4^{2-} ions (Figures S32 and S33).

Structural Descriptions of 2-4

Crystals of **2-4** were obtained from the crystallization of the bulk extracts from DMSO. The data collection and refinement details, hydrogen-bonding tables, and space-fill models of all four complexes are provided in the Supporting Information (Tables S1-S5, Figure S26). A comprehensive overview of the structural features of the crystals of **2-4** is provided here. All three complexes form dimeric capsular assemblies upon tetrahedral oxyanion encapsulation (Figure 10). Remarkable similarities are found between the structural features of **2** and **4**. Both **2** and **4** crystallize in

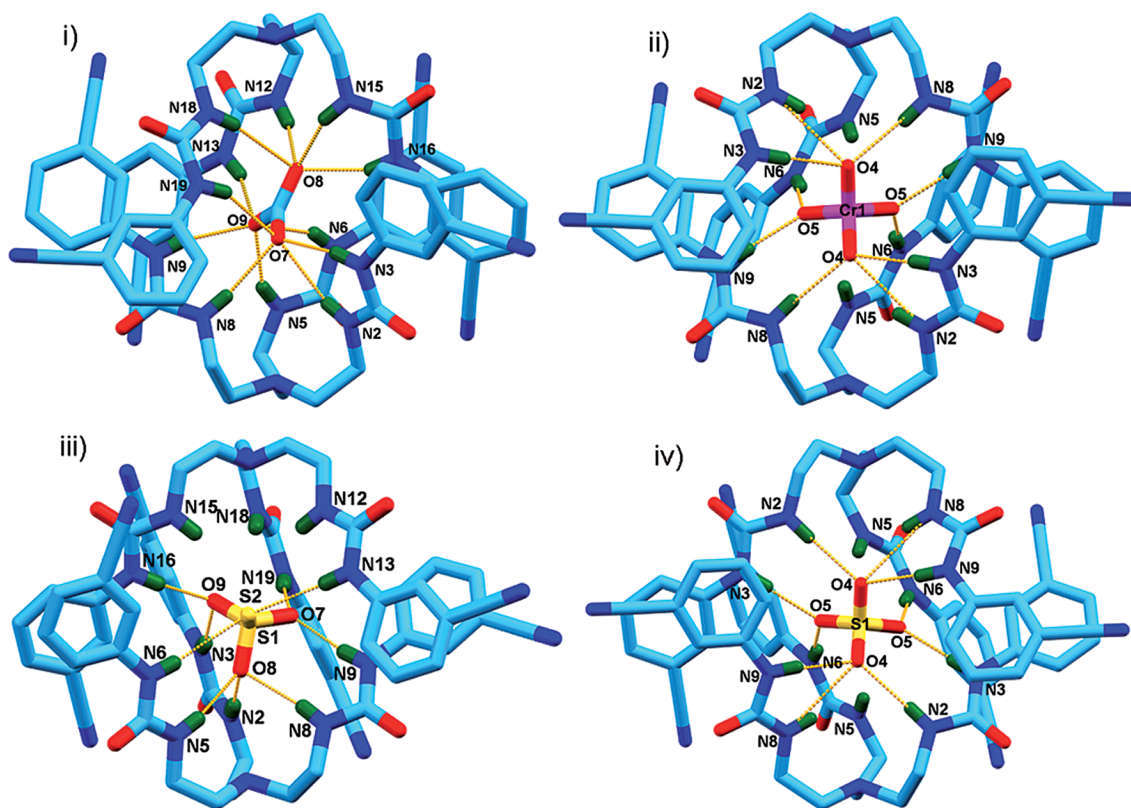


Figure 10. Perspective views of the crystal structures of (i) **1**, (ii) **2**, (iii) **3**, and (iv) **4**. All four complexes show anion-assisted dimeric assemblies of **L1** with multiple N–H...X (X = O, S) interactions (nonacidic hydrogen atoms and counteranions are omitted for clarity).

the monoclinic crystal system in the $C2/c$ space group. The capsular dimensions of the dimeric assembly are measured as 9.70 and 9.71 Å for **2** and **4**, respectively (Table 1). This suggests that the capsular assembly is rigid despite the differences in size of the encapsulated SO_4^{2-} (S–O = 1.47 Å) and CrO_4^{2-} ions (Cr–O = 1.64 Å) in **4** and **2**, respectively. In both cases, the XO_4^{2-} (X = S, Cr) encapsulation is assisted by ten strong N–H...O interactions ($d_{\text{N}\cdots\text{O}} < 3.2$ Å and $\angle\text{N–H}\cdots\text{O} > 140^\circ$). Two oxygen atoms of the XO_4^{2-} ion (X = S, Cr) form three N–H...O bonds, whereas the remaining two oxygen atoms form two N–H...O contacts. The N...O bond lengths of the ten N–H...O contacts in **2** range from 2.82 to 3.02 Å, and the N–H...O angles range from 152 to 171° (Table S3). The N...O bond lengths of the ten N–H...O contacts of **4** vary from 2.83 to 3.04 Å, and the N–H...O bond angles vary from 152 to 172° (Table S5). Notably, the dimension of the dimeric assembly of **4** (9.71 Å) is slightly lower than that of the Ag_2SO_4 -assisted dimeric assembly (9.84 Å) of **L1**.^[7b] Complex **3** with an encapsulated $\text{S}_2\text{O}_3^{2-}$ ion crystallizes in the monoclinic crystal system in the $P2_1/n$ space group. The dimeric assembly of **L1** in **3** is assisted by seven N–H...O interactions and two N–H...S interactions (Figure 10). Of the three oxygen atoms of the encapsulated $\text{S}_2\text{O}_3^{2-}$ ion, two (O7 and O9) are involved in two N–H...O interactions each, and the remaining O8 atoms form three N–H...O contacts. The N...O bond lengths of the seven N–H...O contacts range from 2.79 to 3.08 Å, and the N–H...O angles vary from 158 to 172°. The

S2 atom of the encapsulated $\text{S}_2\text{O}_3^{2-}$ ions forms two N–H...S contacts, namely, N6–H6...S2 ($d_{\text{N}\cdots\text{S}} = 3.51$ Å, $\angle\text{N–H}\cdots\text{S} = 163^\circ$) and N13–H13...S2 ($d_{\text{N}\cdots\text{S}} = 3.41$ Å, $\angle\text{N–H}\cdots\text{S} = 170^\circ$; Table S4). The capsular dimension of the dimeric assembly (9.61 Å) of **3** is quite similar to those of **2** and **4** (Table 1).

Table 1. Capsular dimension of dimeric assemblies and total number of N–H...X interactions present.

Complex	Composition	N–H...X interactions ^[a]	Capsular dimension [Å]
1	$[(\text{L1})_2 \cdot (\text{CO}_3) \cdot (\text{TBA})_2]$	12	9.62
2	$[(\text{L1})_2 \cdot (\text{CrO}_4) \cdot (\text{TBA})_2]$	10	9.70
3	$[(\text{L1})_2 \cdot (\text{S}_2\text{O}_3) \cdot (\text{TBA})_2]$	9	9.61
4	$[(\text{L1})_2 \cdot (\text{SO}_4) \cdot (\text{TBA})_2]$	10	9.71
Ref. ^[7b]	$[(\text{L1})_2 \cdot (\text{Ag})_2 \cdot (\text{SO}_4)]$	12	9.84

[a] X = O for **1**, **2**, and **4**; X = O/S for **3**.

Conclusions

We have established **L1** for the efficient encapsulation of CO_3^{2-} ions through the fixation of aerial CO_2 in basic DMSO solution. The crystal structure of **1** shows the encapsulation of a CO_3^{2-} ion inside the dimeric capsular assembly of **L1** through twelve N–H...O hydrogen-bonding interactions. Complex **1** was successfully employed for the L–L extraction of environmentally relevant anions such as CrO_4^{2-} , $\text{S}_2\text{O}_3^{2-}$, and SO_4^{2-} from water by an anion-ex-

change technique that overcomes their high hydration energies. This is the first report on the L–L extraction of CrO_4^{2-} and $\text{S}_2\text{O}_3^{2-}$ ions from water by an anion-exchange technique. In all three cases, ca. 90% extraction of anions is achieved by L–L extraction with **1**. Further, complex **1** was successfully employed for the extraction of SO_4^{2-} ions from water under highly alkaline conditions and in the presence of excess NO_3^- ions. The crystal structures of all of the isolated anion complexes reveal anion-assisted dimeric capsular assemblies of **L1** of similar capsular dimensions.

Experimental Section

[(L1)₂·(CO₃)·(TBA)₂] (1): **L1** (40 mg) was dissolved in DMSO (10 mL), and an excess of tetrabutylammonium hydroxide (TBAOH) was added. The mixture was stirred and warmed to 60 °C for 10 min and then kept in open air for crystallization. Within 48 h, diamond-shaped colorless crystals of **1** were isolated in high yield (85%). ¹H NMR (300 MHz, [D₆]DMSO): δ = 10.27 (3 H, NH_a), 7.80 (3 H, NH_b), 7.58 (3 H, Ar-CH), 7.51–7.56 (3 H, Ar-CH), 7.05–7.06 (3 H, Ar-CH), 3.21–3.12 (14 H, CH_d merged with CH_a), 2.54–2.51 (6 H, CH_c), 1.51–1.61 (8 H, CH_β), 1.26–1.36 (8 H, CH_γ), 0.90–0.95 (12 H, CH_δ) ppm. ¹³C NMR (75 MHz, [D₆]DMSO): δ = 169.72 (CO₃²⁻), 155.63 (C=O), 142.18 (Ar-C), 129.6 (Ar-C), 124.16 (Ar-C), 122.37 (Ar-C), 120.42 (Ar-C), 119.49 (Ar-C), 111.46 (CN), 58.14 (NCH₂CH₂CH₂CH₃), 54.15 (NCH₂CH₂), 37.49 (NCH₂CH₂), 23.67 (NCH₂CH₂CH₂CH₃), 19.82 (NCH₂CH₂CH₂CH₃), 14.08 (NCH₂CH₂CH₂CH₃) ppm.

General Procedure for Liquid–Liquid (L–L) extraction: In a typical L–L extraction experiment, **1** (30 mg) was dissolved in dichloromethane (5 mL), and a deionized water (5 mL) solution containing 10 equiv. of the respective salt was added. The biphasic solution was then stirred for 6 h and then settled for 15 min. The separated organic layer was then filtered through a Whatman IPS filter paper and evaporated under reduced pressure. Finally, the bulk extract was recrystallized from DMSO. The obtained crystals were then characterized by IR spectroscopy, ¹H and ¹³C NMR spectroscopy, and single-crystal X-ray diffraction analysis. The characterization data of **2–4** are provided below. The yields of **2–4** obtained by the crystallization of the bulk extracts are provided.

[(L1)₂·(CrO₄)·(TBA)₂] (2): Yield: 92%. ¹H NMR (300 MHz, [D₆]DMSO): δ = 9.433 (3 H, NH_a), 7.89 (3 H, Ar-CH), 7.65 (3 H, Ar-CH), 7.18–7.24 (6 H, Ar-CH and NH_b), 3.13–3.18 (14 H, CH_a and CH_d merged), 2.49–2.50 (6 H, CH_c), 1.54–1.56 (8 H, CH_γ), 1.27–1.34 (8 H, CH_β), 0.90–0.95 (12 H, CH_δ) ppm. ¹³C NMR (75 MHz, [D₆]DMSO): δ = 154.93 (C=O), 141.68 (Ar-C), 129.34 (Ar-C), 123.77 (Ar-C), 122.13 (Ar-C), 120.06 (Ar-C), 118.94 (Ar-C), 111.01 (CN), 57.49 (NCH₂CH₂CH₂CH₃), 54.01 (NCH₂CH₂), 37.38 (NCH₂CH₂), 23.01 (NCH₂CH₂CH₂CH₃), 19.15 (NCH₂CH₂CH₂CH₃), 13.41 (NCH₂CH₂CH₂CH₃) ppm.

[(L1)₂·(S₂O₃)·(TBA)₂] (3): Yield: 88%. ¹H NMR (300 MHz, [D₆]DMSO): δ = 9.34 (3 H, NH_a), 7.94 (3 H, Ar-CH), 7.64–7.68 (3 H, Ar-CH), 7.28–7.33 (3 H, Ar-CH), 7.22–7.24 (3 H, Ar-CH), 6.88 (3 H, NH_b), 3.13–3.18 (14 H, CH_d merged with CH_a), 2.51–2.53 (6 H, CH_c), 1.51–1.56 (8 H, CH_β), 1.24–1.36 (8 H, CH_γ), 0.90–0.95 (12 H, CH_δ) ppm. ¹³C NMR (75 MHz, [D₆]DMSO): δ = 155.07 (C=O), 141.71 (Ar-C), 129.59 (Ar-C), 123.96 (Ar-C), 122.20 (Ar-C), 120.07 (Ar-C), 119.01 (Ar-C), 111.14 (CN), 57.49 (NCH₂CH₂CH₂CH₃), 53.91 (NCH₂CH₂), 37.44 (NCH₂CH₂), 23.02 (NCH₂CH₂CH₂CH₃), 19.17 (NCH₂CH₂CH₂CH₃), 13.44 (NCH₂CH₂CH₂CH₃) ppm.

[(L1)₂·(SO₄)·(TBA)₂] (4): Yield: 85%. ¹H NMR (300 MHz, [D₆]DMSO): δ = 9.46 (3 H, NH_a), 7.77 (3 H, Ar-CH), 7.57–7.60 (3 H, Ar-CH), 7.24 (3 H, NH_b), 7.13 (3 H, Ar-CH), 3.13–3.32 (14 H, CH_d merged with CH_a), 2.51–2.54 (6 H, CH_c), 1.51–1.61 (8 H, CH_β), 1.24–1.36 (8 H, CH_γ), 0.90–0.99 (12 H, CH_δ) ppm. ¹³C NMR (75 MHz, [D₆]DMSO): δ = 154.91 (C=O), 141.61 (Ar-C), 129.24 (Ar-C), 123.74 (Ar-C), 121.87 (Ar-C), 119.90 (Ar-C), 118.91 (Ar-C), 110.98 (CN), 57.50 (NCH₂CH₂CH₂CH₃), 54.09 (NCH₂CH₂), 37.08 (NCH₂CH₂), 23.03 (NCH₂CH₂CH₂CH₃), 19.18 (NCH₂CH₂CH₂CH₃), 13.45 (NCH₂CH₂CH₂CH₃) ppm.

Crystallographic Data for 1: C₉₃H₁₃₂N₂₂O₉, M_r = 1702.21 g mol⁻¹, monoclinic, space group P2₁/c, a = 23.599(4) Å, b = 12.574(2) Å, c = 32.380(6) Å, α = 90°, β = 98.635(5)°, γ = 90°, V = 9499(3) Å³, Z = 4, ρ_{calcd.} = 1.19 g cm⁻³, μ = 0.079 mm⁻¹, T = 150(2) K, 43915 reflections, 7009 independent (R_{int} = 0.0662), 5188 observed reflections [I ≥ 2σ(I)], 1125 refined parameters, R1 = 0.0434, wR2 = 0.1088, GOF = 1.013.

Crystallographic Data for 2: C₉₂H₁₃₂N₂₂O₁₀Cr, M_r = 1758.2 g mol⁻¹, monoclinic, space group C2/c, a = 23.396(3) Å, b = 12.7927(15) Å, c = 32.578(4) Å, α = 90°, β = 94.871(4)°, γ = 90°, V = 9715(2) Å³, Z = 4, ρ_{calcd.} = 1.202 g cm⁻³, μ = 0.184 mm⁻¹, T = 150(2) K, 25959 reflections, 5520 independent (R_{int} = 0.1246), 3816 observed reflections [I ≥ 2σ(I)], 568 refined parameters, R1 = 0.0799, wR2 = 0.2648, GOF = 1.127.

Crystallographic Data for 3: C₉₂H₁₃₂N₂₂O₉S₂, M_r = 1754.34 g mol⁻¹, monoclinic, space group P2₁/n, a = 23.9868(16) Å, b = 13.5376(9) Å, c = 30.130(2) Å, α = 90°, β = 94.405(2)°, γ = 90°, V = 9755.0(11) Å³, Z = 4, ρ_{calcd.} = 1.194 g cm⁻³, μ = 0.012 mm⁻¹, T = 150(2) K, 42880 reflections, 9051 independent (R_{int} = 0.1247), 5722 observed reflections [I ≥ 2σ(I)], 1135 refined parameters, R1 = 0.0791, wR2 = 0.2447, GOF = 1.059.

Crystallographic Data for 4: C₉₂H₁₃₂N₂₂O₁₀S, M_r = 1738.27 g mol⁻¹, monoclinic, space group C2/c, a = 23.428(2) Å, b = 12.8969(13) Å, c = 32.641(3) Å, α = 90°, β = 95.256(2)°, γ = 90°, V = 9821.0(16) Å³, Z = 4, ρ_{calcd.} = 1.176 g cm⁻³, μ = 0.099 mm⁻¹, T = 150(2) K, 42171 reflections, 7817 independent (R_{int} = 0.0681), 5691 observed reflections [I ≥ 2σ(I)], 568 refined parameters, R1 = 0.0455, wR2 = 0.1135, GOF = 1.008.

CCDC-887538 (for **1**), -973806 (for **2**), -973807 (for **3**), and -887539 (for **4**) contain the supplementary crystallographic data for this paper. These data can be obtained free of charge from The Cambridge Crystallographic Data Centre via www.ccdc.cam.ac.uk/data_request/cif.

Supporting Information (see footnote on the first page of this article): ¹H and ¹³C NMR spectra, IR spectra, space-fill models, details of hydrogen bonds.

Acknowledgments

P. G. gratefully acknowledges the Department of Science and Technology (DST), New Delhi for financial support through a Swarnajayanti Fellowship. R. D. and S. C. acknowledge the Indian Association for the Cultivation of Science (IACS), Kolkata for research fellowships. The single-crystal X-ray diffraction data were collected at the DBT-funded CEIB program (project number BT/01/CEIB/11/V/13) awarded to the Department of Organic Chemistry, IACS, Kolkata.

[1] a) A. Zhitkovich, *Chem. Res. Toxicol.* **2011**, *24*, 1617–1629; b) A. D. Dayan, A. J. Paine, *Human Experimental Toxicol.* **2001**,

- 20, 439–451; c) C. Oze, D. K. Bird, S. Fendorf, *Proc. Natl. Acad. Sci. USA* **2007**, *104*, 6544–6549; d) D. Blowes, *Science* **2002**, *295*, 2024–2025.
- [2] *Guidelines for Drinking Water Quality*, vol. 1: *Recommendations*, World Health Organization, Geneva, Switzerland, **1993**.
- [3] B. A. Moyer, R. Custelcean, B. P. Hay, J. L. Sessler, K. Bowman-James, V. W. Day, S.-O. Kang, *Inorg. Chem.* **2013**, *52*, 3473–3490, and references cited therein.
- [4] a) M. G. Aylmore, D. M. Muir, *Miner. Eng.* **2001**, *14*, 135–174; b) A. H. Hall, R. Dart, G. Bogda, *Ann. Emerg. Med.* **2007**, *49*, 806–813.
- [5] a) R. Banerjee, A. Phan, B. Wang, C. Knobler, H. Furukawa, M. O’Keeffe, O. M. Yaghi, *Science* **2008**, *319*, 939–943; b) G. T. Rochelle, *Science* **2009**, *325*, 1652–1654; c) Y. Jin, B. A. Voss, A. Jin, H. Long, R. D. Noble, W. Zhang, *J. Am. Chem. Soc.* **2011**, *133*, 6650–6658; d) T. Mitra, X. Wu, R. Clowes, J. T. A. Jones, K. E. Jelfs, D. J. Adams, A. Trewin, J. Bacsá, A. Steiner, A. I. Cooper, *Chem. Eur. J.* **2011**, *17*, 10235–10240; e) J. M. Simmons, H. Wu, W. Zhou, T. Yildirim, *Energy Environ. Sci.* **2011**, *4*, 2177–2185; f) S. Dalapati, S. Jana, R. Saha, M. A. Alam, N. Guchhait, *Org. Lett.* **2012**, *14*, 3244–3247.
- [6] a) S. J. Brooks, P. A. Gale, M. E. Light, *Chem. Commun.* **2006**, 4344–4346; b) S. J. Brooks, S. E. Garcia-Garrido, M. E. Light, P. A. Cole, P. A. Gale, *Chem. Eur. J.* **2007**, *13*, 3320–3329.
- [7] a) T. Gunnlaugsson, P. E. Kruger, P. Jensen, F. M. Pfeffer, G. M. Husse, *Tetrahedron Lett.* **2003**, *44*, 8909–8913; b) I. Ravikumar, P. Ghosh, *Chem. Commun.* **2010**, *46*, 1082–1084; c) S. K. Dey, R. Chutia, G. Das, *Inorg. Chem.* **2012**, *51*, 1727–1738.
- [8] a) F. Hofmeister, *Arch. Exp. Pathol. Pharmacol.* **1888**, *24*, 247–260; b) Y. J. Marcus, *J. Chem. Soc. Faraday Trans.* **1991**, *87*, 2995–2999.
- [9] a) A. K. Chakravarti, S. B. Chowdhury, S. Chakrabarty, T. Chakrabarty, D. C. Mukherjee, *Colloids Surf. A* **1995**, *103*, 59–71; b) S. V. Prasanna, P. V. Kamath, *Solid State Sci.* **2008**, *10*, 260–266; c) P. A. Kumar, M. Ray, S. Chakraborty, *J. Hazard. Mater.* **2007**, *143*, 24–32; d) Y. Watanabe, T. Suzuki, K. Kimura, *Water Sci. Technol.* **2000**, *41*, 9–16.
- [10] a) M. Bayrakci, Ş. Ertul, M. Yilmaz, *Tetrahedron* **2009**, *65*, 7963–7968; b) S. Sayin, M. J. Yilmaz, *J. Chem. Eng. Data* **2011**, *56*, 2020–2029.
- [11] R. Custelcean, P. V. Bonnesen, N. C. Duncan, X. Zhang, L. A. Watson, G. V. Berkel, W. B. Parson, B. P. Hay, *J. Am. Chem. Soc.* **2012**, *134*, 8525–8534.
- [12] T. Shioya, S. Nishizawa, N. Teramae, *J. Am. Chem. Soc.* **1998**, *120*, 11534–11535.
- [13] I. Ravikumar, P. Ghosh, *Chem. Soc. Rev.* **2012**, *41*, 3077–3098.
- [14] a) L. R. Eller, M. Stepien, C. J. Fowler, J. T. Lee, J. L. Sessler, B. A. Moyer, *J. Am. Chem. Soc.* **2007**, *129*, 11020–11021; b) C. J. Fowler, T. J. Haverlock, B. A. Moyer, J. A. Shriver, D. E. Gross, M. Marquez, J. L. Sessler, M. A. Hossain, K. Bowman-James, *J. Am. Chem. Soc.* **2008**, *130*, 14386–14387.
- [15] a) C. Jia, B. Wu, S. Li, X. Huang, Q. Zhao, Q. S. Li, X. J. Yang, *Angew. Chem. Int. Ed.* **2011**, *50*, 486–490; *Angew. Chem.* **2011**, *123*, 506; b) P. Bose, R. Dutta, S. Santra, B. Chowdhury, P. Ghosh, *Eur. J. Inorg. Chem.* **2012**, 5791–5801.
- [16] B. Akhuli, I. Ravikumar, P. Ghosh, *Chem. Sci.* **2012**, *3*, 1522–1530.
- [17] a) C. Raposo, M. Almaraz, M. Martín, V. Weinrich, M. L. Mussóns, V. Alcázar, M. C. Caballero, J. R. Morán, *Chem. Lett.* **1995**, 759–760; b) R. Custelcean, B. A. Moyer, B. P. Hay, *Chem. Commun.* **2005**, 5971–5973; c) D. A. Jose, D. K. Kumar, B. Ganguly, A. Das, *Inorg. Chem.* **2007**, *46*, 5817–5819; d) P. S. Lakshminarayanan, I. Ravikumar, E. Suresh, P. Ghosh, *Chem. Commun.* **2007**, 5214–000; e) B. Wu, J. Liang, J. Yang, C. Jia, X.-J. Yang, H. Zhang, N. Tang, C. Janiak, *Chem. Commun.* **2008**, 1762–1764; f) R. Custelcean, P. Remy, P. V. Bronnesen, D. Jiang, B. A. Moyer, *Angew. Chem. Int. Ed.* **2008**, *47*, 1866–1870; *Angew. Chem.* **2008**, *120*, 1892; g) I. Ravikumar, P. S. Lakshminarayanan, M. Arunachalam, E. Suresh, P. Ghosh, *Dalton Trans.* **2009**, 4160–4168; h) Y. Li, K. M. Mullen, T. D. W. Claridge, P. J. Costa, V. Felix, P. D. Beer, *Chem. Commun.* **2009**, 7134–7136; i) R. Custelcean, A. Bock, B. A. Moyer, *J. Am. Chem. Soc.* **2010**, *132*, 7177–7185; j) V. Amendola, L. Fabbrizzi, L. Mosca, *Chem. Soc. Rev.* **2010**, *39*, 3889–3915; k) A. Pramanik, B. Thompson, T. Hayes, K. Tucker, D. R. Powell, P. V. Bonnesen, E. D. Ellis, K. S. Lee, H. Yu, M. A. Hossain, *Org. Biomol. Chem.* **2011**, *9*, 4444–4447; l) N. Busschaert, M. Wenzel, M. E. Light, P.-I. Hernández, R.-P. Tomás, P. A. Gale, *J. Am. Chem. Soc.* **2011**, *133*, 14136–14148; m) M. Li, B. Wu, C. Jia, X. Huang, Q. Zhao, S. Shao, X. J. Yang, *Chem. Eur. J.* **2011**, *17*, 2272–2280; n) A. Rajbanshi, B. A. Moyer, R. Custelcean, *Cryst. Growth Des.* **2011**, *11*, 2702–2706; o) A. Basu, G. Das, *Dalton Trans.* **2012**, *41*, 10792–10802; p) P. Bose, R. Dutta, P. Ghosh, *Org. Biomol. Chem.* **2013**, *11*, 4581–4584; q) R. Dutta, P. Bose, P. Ghosh, *Dalton Trans.* **2013**, *42*, 11371–11374; r) R. Custelcean, *Chem. Commun.* **2013**, *49*, 2173–2182.
- [18] M. J. Hynes, *J. Chem. Soc., Dalton Trans.* **1993**, 311–312.

Received: March 5, 2014

Published Online: July 21, 2014